EPJ D
Atomic, Molecular, Optical and Plasma Physics
EPJ.org
your physics journal

Eur. Phys. J. D **63**, 463–472 (2011) DOI: 10.1140/epjd/e2011-10729-8

Programmed discrimination of qbits with added classical information

A.J.T. Colin, S.M. Barnett and J. Jeffers

EDP SCIENCES
Società Italiana di Fisica
Springer

Eur. Phys. J. D **63**, 463–472 (2011)
DOI: 10.1140/epjd/e2011-10729-8

THE EUROPEAN PHYSICAL JOURNAL D

Regular Article

Programmed discrimination of qbits with added classical information

A.J.T. Colin[a], S.M. Barnett, and J. Jeffers

Department of Physics, Scottish Universities Physics Alliance, Strathclyde University, John Anderson Building, 107 Rottenrow, Glasgow G4 0NG, UK

Received 29 December 2010 / Received in final form 14 March 2011
Published online 17 June 2011 – © EDP Sciences, Società Italiana di Fisica, Springer-Verlag 2011

Abstract. We investigate some properties of programmed quantum-state discriminators with simple programs. Bergou et al. [Phys. Rev. A **73**, 062334 (2006)] have considered programmable devices which are supplied with two distinct but unknown *program* qbits and one *data* qbit which is certain to be identical to one or other of the program qbits. The task is to discriminate between the first and the second possibility. In this paper, we consider this state-discrimination problem when there is some additional classical information available. We find that in the minimum error discrimination mode, the probability of correct discrimination is increased by each type of classical information. The same is broadly true of unambiguous discrimination, with the chance of success improving when the overlap between the program qbits is reduced.

1 Introduction

The earliest classical computing machines were designed to carry out fixed functions, such as multiplication and calculation of square roots, by mechanical means. A major step in their evolution occurred when Charles Babbage [2] designed the analytical engine, a machine that could be adapted to carry out a wide range of different functions, using a fixed mechanism and supplied with a set of instructions as *data*. This is the fundamental configuration used in all present-day (classical) computers.

It might be that quantum computers will follow a similar line of evolution. Every system proposed at present depends on hardware dedicated to solving one specific problem such as searching or factorisation. Designs for general-purpose quantum computers have yet to be developed.

The term *programmable quantum computer* has received two different interpretations. On one understanding, it relates to *universal* quantum gates that can be switched, by classical control inputs, to perform a flexible range of different functions. Significant advances in this area have already been reported [3]. The other understanding refers to assemblies of gates whose combined unitary function is controlled entirely by quantum inputs, so retaining the adaptability of a general-purpose computer without the need to carry out measurements of intermediate results. It is this latter interpretation that is of interest here.

Much of the published work to date has been done by Bergou et al. [1]. This present paper advances some of their ideas, by considering the behaviour of certain multi-qbit quantum systems restricted by known relations between the qbits.

2 Background

A key aspect of quantum information technology is the ability to measure the states of individual quantum systems. Unlike the case with classical systems, there are strict limits to the accuracy that such measurements can be made.

Every measurement of a quantum system with a density operator $\hat{\rho}$ corresponds to a set of operators $\{\hat{\pi}_n\}$ for $n = 1, 2, 3\ldots$ such that the probability of outcome $P(j)$ is $\mathrm{Tr}(\hat{\rho}\hat{\pi}_\mathrm{j})$. As *some* outcome is certain, the operators sum to the unit operator $\hat{I}$. If the $\hat{\pi}$ operators form an orthonormal set they represent a von Neumann measurement. In this case, a system prepared in an eigenstate of the associated observable will give a predictable result. More generally, the measurement will be a generalised one and the result will typically be probabilistic irrespective of the state in which the system was prepared.

For any given system, it is generally possible to find sets of operators, called probability operator measures ('POM's for short) [4], which can be optimised in various ways [5]. In general the probability operators $\hat{\pi}_i$ will not be orthogonal:

$$\hat{\pi}_i\hat{\pi}_j \neq \hat{\pi}_i\delta_{ij}. \quad (1)$$

[a] e-mail: andrew@crm.scotnet.co.uk

The POM formalism has been especially important in the problem of quantum state-discrimination. Optimal POMs fall into two distinct categories. The *minimum error* POM has one element for each possible state of the quantum system, and each outcome carries a probability of error. By comparing the (known) statistical expectation of the states with the probability given by each element in the POM, we can find an average error rate in the discrimination between the possible states. On the other hand the *unambiguous discrimination* POM has an additional operator, $\hat{\pi}_0$, that corresponds to 'state unknown'. If a state is recognised at all, the outcome is certain; there is no doubt at all that the system is in that state. However, recognition may fail completely. The expression

$$P(0) = \mathrm{Tr}(\hat{\rho}\hat{\pi}_0) \tag{2}$$

gives the probability that failure to discriminate occurs. We buy occasional certainty in discrimination at the cost of frequent total ambiguity.

Measurements do not necessarily need to be applied to systems such as single qbits. They can also be used to discover relationships between sets of qbits (for example, whether two qbits are the same) without probing their actual values. A simple example, closely related to the problem of interest, is the comparison of two systems each prepared in an unknown state [6,7].

Several different configurations of quantum systems have been considered as information carriers. The simplest arrangement consists of a single system, such as a polarised photon or isolated atom, where the states can be described as unit vectors in an N-dimensional Hilbert space. The system carries a single digit of radix N, with the several possible values being represented by *orthogonal* vectors, which we call 'basis states'. If $N = 2$ then we have a two-state system or *qbit* [8].

If the basis states are orthogonal, they can be recognised without error by a von Neumann measurement. If the system is in a superposition of two or more orthogonal basis states, the von Neumann measurement will yield a probabilistic result. The theory of von Neumann measurements has been understood since the publication of von Neumann's book in 1932 [9].

Another arrangement also consists of a single quantum system, but here the possible states are deliberately made *non-orthogonal* to one another. No measurement can distinguish the states with perfect fidelity. This fact is made the basis of secure data transmission protocols, where the presence of any eavesdropper will inevitably be detected. The identification of non-orthogonal states has been intensively researched by Barnett et al. [6], Sedlak et al. [10], Kleinmann et al. [11].

A third arrangement, which has been considered recently, uses *three* quantum systems to represent a single binary digit. Two of the systems, **A** and **C**, are called the 'program qbits'. They are prepared in the states $|\psi_1\rangle$ and $|\psi_3\rangle$, respectively. The third qbit **B**, known as the 'data qbit', is *guaranteed* to be in the state $|\psi_1\rangle$, representing 0, or $|\psi_3\rangle$, representing 1. The discrimination problem consists of deciding which of these two possibilities is true and so retrieving the bit value.

This arrangement would be useful in setting up communication between two remote stations where there is no prior agreement on the identity of the basis states. This is because the arrangement is insensitive to any unitary transformation, so long as it applies to all the qbits identically.

The error rate of such a hypothetical device, using both *minimum error* and *unambiguous discrimination* POMs, has been investigated by Bergou et al. [1]. We refer to these five authors as the 'Hunter Group', after the college at which two of the authors are based. They assume that the two program qbits are completely unrelated, and find an average expected error rate when the program qbits are equally likely to be anywhere on the surface of the Bloch sphere.

In this paper, we refer to the set of three qbits **A**, **B** and **C**, prepared in the states $\{|\psi_1\rangle_A, |\psi_2\rangle_B, |\psi_3\rangle_C\}$ as a *Triad*, where the subscripts {A,B,C} identify the position of the qbits in the Triad state, with the data qbit **B** placed between the other two. The state $|\psi_2\rangle$ will, of course, be either $|\psi_1\rangle$ or $|\psi_3\rangle$. We consider the effect on the average error rate of additional classical (i.e., certain) information. The extra information appears as constraints on the values of the two program qbits. We consider three specific cases in particular:

- A known overlap between the two program qbits.
- The knowledge that both program qbits lie on a *given* great circle on the Bloch sphere.
- The knowledge that one program qbit is restricted to a cap centered on the north pole of the Bloch sphere, and the other to a similar cap centered on the south pole.

We also take into account the effect of different a priori probabilities of the two outcomes.

3 The computational method used by the Hunter group

Our calculations have much in common with those used by the group of authors in [1]. In this section we give an outline of their methods.

Consider a Triad. As $|\psi_2\rangle$ must be the same as either $|\psi_1\rangle$ or $|\psi_3\rangle$, there are only two possibilities for the input state of the discrimination device:

$$|\Psi_1^{in}\rangle = |\psi_1\rangle_A|\psi_1\rangle_B|\psi_3\rangle_C$$
$$|\Psi_2^{in}\rangle = |\psi_1\rangle_A|\psi_3\rangle_B|\psi_3\rangle_C. \tag{3}$$

As both $|\psi_1\rangle$ and $|\psi_3\rangle$ are unknown, the Hunter group finds two density matrices, both averaged over the Bloch sphere:

$$\overline{\hat{\rho}}_1 = \overline{|\Psi_1^{in}\rangle\langle\Psi_1^{in}|}$$
$$\overline{\hat{\rho}}_2 = \overline{|\Psi_2^{in}\rangle\langle\Psi_2^{in}|}. \tag{4}$$

The states $|\psi_1\rangle$ and $|\psi_3\rangle$ are independent of one another, so $\overline{\hat{\rho}}_1$ can be written as the tensor product $\overline{\hat{\lambda}}_1 \otimes \overline{\hat{\mu}}_1$, where

$$\overline{\hat{\lambda}}_1 = \overline{|\psi_1\rangle|\psi_1\rangle\langle\psi_1|\langle\psi_1|}$$

$$\overline{\hat{\mu}}_1 = \overline{|\psi_3\rangle\langle\psi_3|}. \tag{5}$$

Both $\overline{\hat{\lambda}}_1$ and $\overline{\hat{\mu}}_1$ are averaged over the whole Bloch sphere.

For a general qbit $|\psi_1\rangle = \cos(\beta/2)|0\rangle + e^{i\alpha}\sin(\beta/2)|1\rangle$, the product state is the four-component vector:

$$|\psi_1\rangle|\psi_1\rangle = (\cos(\beta/2)|0\rangle + e^{i\alpha}\sin(\beta/2)|1\rangle)^{\otimes 2}$$

$$= \begin{pmatrix} & \cos^2(\beta/2) & |00\rangle \\ +e^{i\alpha} & \sin(\beta/2)\cos(\beta/2) & |01\rangle \\ +e^{i\alpha} & \sin(\beta/2)\cos(\beta/2) & |10\rangle \\ +e^{2i\alpha} & \sin^2(\beta/2) & |11\rangle \end{pmatrix} \tag{6}$$

so that $\overline{\hat{\lambda}}_1$ is the 4×4 matrix which is the tensor product of this vector and its complex conjugate, where each element is averaged over the Bloch sphere. Computing this average gives:

$$\overline{\hat{\lambda}}_1 = \frac{1}{4\pi}\int_0^{2\pi} d\alpha \int_0^{\pi} d\beta |\psi_1\rangle|\psi_1\rangle\langle\psi_1|\langle\psi_1|$$

$$= \frac{1}{6}\begin{pmatrix} 2&0&0&0 \\ 0&1&1&0 \\ 0&1&1&0 \\ 0&0&0&2 \end{pmatrix}, \tag{7}$$

where the rows and columns correspond, in order, to the states $|00\rangle$, $|01\rangle$, $|10\rangle$ and $|11\rangle$.

Alternatively, $|\Psi^{in}\rangle$ is *symmetrical* in the two components $|\psi_1\rangle_A|\psi_1\rangle_B$. $\overline{\hat{\lambda}}_1$ can be expressed in the normalised form

$$\overline{\hat{\lambda}}_1 = \frac{1}{3}\left(\hat{\mathbf{I}} - |\psi^-\rangle\langle\psi^-|\right) \tag{8}$$

where $|\psi^-\rangle$ is the antisymmetric Bell state, so that $\overline{\hat{\lambda}}_1$ is proportional to the projector on to the symmetric two-qbit subspace.

A similar calculation shows that $\overline{\hat{\mu}}$ is proportional to the identity operator:

$$\overline{\hat{\mu}}_1 = \frac{1}{4\pi}\int_0^{2\pi} d\alpha \int_0^{\pi} d\beta |\psi_3\rangle\langle\psi_3|$$

$$= \frac{1}{2}\begin{pmatrix} 1&0 \\ 0&1 \end{pmatrix}. \tag{9}$$

Tensor multiplication of these gives

$$\overline{\hat{\rho}}_1 = \overline{\hat{\lambda}}_1 \otimes \overline{\hat{\mu}}_1. \tag{10}$$

This density matrix applies to the first of the two states, where the first and the second qbits are identical. Similarly, if the second and third qbits are identical,

$$\overline{\hat{\rho}}_2 = \overline{\hat{\mu}}_1 \otimes \overline{\hat{\lambda}}_1. \tag{11}$$

These two density matrices form the basis for calculating optimum error rates for the minimum error strategy. For readers who prefer more detail, the full density matrices are given in Appendix.

3.1 Minimum error

Suppose that η_1 is the a priori probability that the data qbit is the same as $|\psi_1\rangle$, and η_2 the probability that the data qbit is the same as $|\psi_3\rangle$. Clearly, $\eta_1 + \eta_2 = 1$. To find the minimum error the Hunter group compute the difference matrix:

$$\hat{\Lambda} = \left(\eta_1\overline{\hat{\rho}}_1 - \eta_2\overline{\hat{\rho}}_2\right). \tag{12}$$

Following Helstrom [12], the lowest probability of error (P.E.) that can be achieved in the discrimination is given by:

$$\text{P.E.} = \frac{1}{2}(1 - z) \tag{13}$$

where z is the sum of the absolute values of the eigenvalues of $\hat{\Lambda}$. It is worth noting that when $\eta_1 = \eta_2 = 1/2$, so that there is no bias either way, and in the absence of any classical data, P.E. ≈ 0.356. As η_1 tends to 1 (or zero) the probability of error falls accordingly, in a nearly linear way.

3.2 Unambiguous discrimination

The Hunter Group's method is an adaptation of the process described in [13], which we summarise below. The method depends on finding an unambiguous discrimination POM that consists of the set of operators $\{\hat{\pi}_0, \hat{\pi}_1, \hat{\pi}_2\}$ such that $\hat{\pi}_1$ is *orthogonal* to $\hat{\rho}_2$, $\hat{\pi}_2$ is *orthogonal* to $\hat{\rho}_1$, and $\hat{\pi}_0 = I - \hat{\pi}_1 - \hat{\pi}_2$. Possible measurement outcomes mean:

- $\hat{\pi}_1$: the system is certainly in state $\hat{\rho}_1$;
- $\hat{\pi}_2$: the system is undoubtedly in state $\hat{\rho}_2$;
- $\hat{\pi}_0$: no information about the state is available, and the original state is changed by the measurement so that further measurements are useless.

As $\hat{\rho}_1$ is symmetric in qbits $|\psi_1\rangle_A$ and $|\psi_1\rangle_B$, $\hat{\pi}_2$ can simply be a multiple of the projector P_{AB}^{ASYM} on to the (zero) asymmetric sub-state of these two qbits, so that $\langle\Psi_1|\hat{\pi}_2|\Psi_1\rangle = \text{Tr}(\hat{\rho}_1\hat{\pi}_2) = 0$.

This projector is

$$P_{AB}^{ASYM} = |\psi^-\rangle_{AB}{}_{AB}\langle\psi^-| \tag{14}$$

where $|\psi^-\rangle_{AB}$ is the antisymmetric state:

$$|\psi^-\rangle_{AB} = \frac{1}{\sqrt{2}}\left(|\psi_1\rangle_A|\overline{\psi}_1\rangle_B - |\overline{\psi}_1\rangle_A|\psi_1\rangle_B\right). \tag{15}$$

Given that the system is in state $|\Psi_j^{in}\rangle$, $(j = 1, 2)$ the overall probability of correct identification, p_j, is

$$p_j = \langle\Psi_j^{in}|\hat{\pi}_j|\Psi_j^{in}\rangle. \tag{16}$$

Substituting for $\hat{\pi}_j$ in this equation, and simplifying, it can be shown that

$$p_j = c_j/2\left(1 - |\langle\psi_1|\psi_3\rangle|^2\right) \quad (j = 1, 2) \tag{17}$$

where c_1 and c_2 are unknown real positive constants and $\langle\psi_1|\psi_3\rangle$ is the overlap between the two program qbits.

It remains only to find optimum values for c_1 and c_2, while ensuring that $\hat{\pi}_0$ remains a positive operator. The outcome depends on η_1 and η_2, the a priori probabilities that the system is in state $|\Psi_1^{in}\rangle$ or $|\Psi_2^{in}\rangle$. For a broad range, centred on $\eta_1 = 1/2$, the analysis shows that

$$c_1 = \frac{2}{3}\left(2 - \sqrt{\eta_2/\eta_1}\right) \tag{18}$$

$$c_2 = \frac{2}{3}\left(2 - \sqrt{\eta_1/\eta_2}\right). \tag{19}$$

The overall probability of correct unambiguous identification of the qbit is given by

$$P = \eta_1 p_1 + \eta_2 p_2. \tag{20}$$

Substitution from equations (14)–(17) shows that

$$P = \frac{2}{3}\left(1 - \sqrt{\eta_1\eta_2}\right)\left(1 - |\langle\psi_1|\psi_3\rangle|^2\right). \tag{21}$$

For this to be valid both c_1 and c_2 must be non-negative, and this is only true when $\frac{1}{5} \leq \eta_1 \leq \frac{4}{5}$. Outwith this range it is better to use a projective von Neumann measurement aligned with the more frequent possibility. Here the probability of correct discrimination for $\eta_1 > \frac{4}{5}$ is

$$P_{high\ \eta_1} = \frac{1}{2}\eta_1\left(1 - |\langle\psi_1|\psi_3\rangle|^2\right). \tag{22}$$

Conversely, if $\eta_1 < \frac{1}{5}$,

$$P_{low\ \eta_1} = \frac{1}{2}\eta_2\left(1 - |\langle\psi_1|\psi_3\rangle|^2\right). \tag{23}$$

In the case considered by the Hunter group, the position of the program qbits is undefined, and their average overlap is $\frac{1}{\sqrt{2}}$. This leads directly to their formula for failure to make an unambiguous discrimination in the central range of η of

$$Q_F = \frac{2 + \sqrt{\eta_1\eta_2}}{3}. \tag{24}$$

This completes our review of some of the Hunter Group's principal results. They will be fundamental for our own findings, which we report in the following sections of the paper. In particular, we note that the success of unambiguous discrimination depends only on two factors: the a priori frequencies η_1 and η_2, and the overlap between the program qbits.

4 The probability of error with a known overlap between the program qbits

In the sections that follow we shall calculate density matrices $\overline{\hat{\rho}}_1$ and $\overline{\hat{\rho}}_2$, analogous to those used by the Hunter group, but modified to account for the classical information which is available.

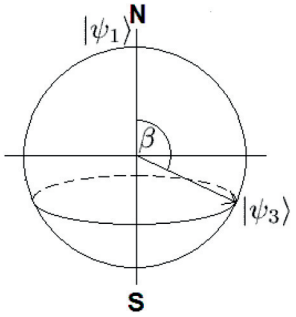

Fig. 1. Bloch sphere with locus of constant overlap with $|0\rangle$.

This part of the paper posits that the two program qbits of the Triad are not completely independent but have a known fixed overlap. The problem is tackled in two stages: firstly we solve a simple case where the position of one of the program qbits is fixed, and secondly, we extend this solution to cover the general situation.

We provisionally place one of the program qbits at the north pole of the Bloch sphere ($|\psi_1\rangle = |0\rangle$). The other program qbit can be now written in the general form

$$|\psi_3\rangle = \cos(\beta/2)|0\rangle + e^{i\alpha}\sin(\beta/2)|1\rangle. \tag{25}$$

The overlap is given by:

$$\begin{aligned}\langle\psi_1|\psi_3\rangle &= \left(\cos(\beta/2)\langle 0|0\rangle + e^{i\alpha}\sin(\beta/2)\langle 0|1\rangle\right)\\ &= \cos(\beta/2).\end{aligned} \tag{26}$$

The overlap is independent of α, as shown in Figure 1. For all values of β except 0 and π, $|\psi_3\rangle$ lies on a circle of latitude given by $(0 \leq \alpha < 2\pi)$.

4.1 Finding density matrices

We first find provisional density matrices $\overline{\hat{\rho}}_{1(prov)}$ and $\overline{\hat{\rho}}_{2(prov)}$ using our *temporary* assumption that one qbit is at the north pole of the Bloch sphere. Taking

$$\begin{aligned}|\psi_1\rangle &= |0\rangle\\ |\psi_3\rangle &= \cos(\beta/2)|0\rangle + e^{i\alpha}\sin(\beta/2)|1\rangle.\end{aligned} \tag{27}$$

Assuming that $|\psi_2\rangle$, the data qbit, is the same as $|\psi_1\rangle$, we get the product ket

$$\begin{aligned}|\Psi_{1(prov)}\rangle &= |\psi_1\rangle|\psi_1\rangle|\psi_3\rangle\\ &= \left(\cos(\beta/2)|000\rangle + e^{i\alpha}\sin(\beta/2)|001\rangle\right).\end{aligned} \tag{28}$$

The provisional density matrix $\overline{\hat{\rho}}_{1(prov)}$ is the value of $|\Psi_{1(prov)}\rangle\langle\Psi_{1(prov)}|$ averaged over the circle of constant overlap. This requires us to average over all values of the azimuthal angle α, which removes the off-diagonal terms, leaving

$$\overline{\hat{\rho}}_{1(prov)} = \cos^2(\beta/2)|000\rangle\langle 000| + \sin^2(\beta/2)|001\rangle\langle 001|. \tag{29}$$

To find $\overline{\hat{\rho}}_{2(prov)}$, where $|\psi_2\rangle = |\psi_3\rangle$, we use a similar argument, but this time placing $|\psi_3\rangle$ at $|0\rangle$, instead of $|\psi_1\rangle$. We obtain

$$\overline{\hat{\rho}}_{2(prov)} = \cos^2(\beta/2)|000\rangle\langle 000| + \sin^2(\beta/2)|100\rangle\langle 100|. \tag{30}$$

Next we generalise this result by removing the restriction that one of the program qbits must be at the north pole. To make the appropriate transformation we replace $|0\rangle$ by the general form

$$|0'\rangle = \cos(\theta/2)|0\rangle + e^{i\psi}\sin(\theta/2)|1\rangle \tag{31}$$

and $|1\rangle$ by the state orthogonal to $|0'\rangle$, namely,

$$|1'\rangle = \sin(\theta/2)|0\rangle - e^{i\psi}\cos(\theta/2)|1\rangle. \tag{32}$$

The generalised forms of $|\Psi_1\rangle$ and $|\Psi_1\rangle$ are now given by

$$|\Psi_1\rangle = \cos(\beta/2)|0'0'0'\rangle + e^{i\alpha}\sin(\beta/2)|0'0'1'\rangle$$

$$|\Psi_2\rangle = \cos(\beta/2)|0'0'0'\rangle + e^{i\alpha}\sin(\beta/2)|1'0'0'\rangle. \tag{33}$$

We can write $|\Psi_1\rangle$ as the sum of two column vectors:

$$|\Psi_1\rangle = |p\rangle + |q_1\rangle \tag{34}$$

where $|p\rangle$ is the expansion, in terms of the computational basis states $|0\rangle$ and $|1\rangle$, of the term $\cos(\beta/2)|0'0'0'\rangle$, and $|q_1\rangle$ is the expansion of $e^{i\alpha}\sin(\beta/2)|0'0'1'\rangle$. Similarly,

$$|\Psi_2\rangle = |p\rangle + |q_2\rangle \tag{35}$$

where $|q_2\rangle$ is the expansion of the term $e^{i\alpha}\sin(\beta/2)|1'0'0'\rangle$. The full forms of these vectors are given in Appendix.

Let **A** denote the outer product $|p\rangle\langle p|$ and **B** denote $|q_1\rangle\langle q_1|$. The density matrix $\overline{\hat{\rho}}_1$ is the average, over the Bloch sphere, of the weighted sum of two matrices **A** and **B**:

$$\overline{\hat{\rho}}_1 = \frac{1}{4\pi}\left(\int_S \mathbf{A}dS + \int_S \mathbf{B}dS\right). \tag{36}$$

The integral $\int_S dS$ denotes integration over the surface of the Bloch sphere.

Similarly, using the definintion of $\overline{\hat{\rho}}_2$ we find

$$\overline{\hat{\rho}}_2 = \frac{1}{4\pi}\left(\int_S \mathbf{A}dS + \int_S \mathbf{C}dS\right) \tag{37}$$

where **C** is the outer product $|q_2\rangle\langle q_2|$. For completeness, the expanded forms of these integrals are given in Appendix.

We complete the computation, and work out the expected probable error for various values of the a priori probability η_1 and the overlap measure β using Helstrom's expression (13). For most values of η_1 and β it is convenient to use a computer, but in the simplest case, for $\eta_1 = \eta_2 = 0.5$ and $\beta = \pi$ an analytic solution is readily accessible. For these values P.E. ≈ 0.211.

Figure 2 presents a set of results for the error rate expected from Triads with various degrees of overlap between the program qbits and a range of values for the

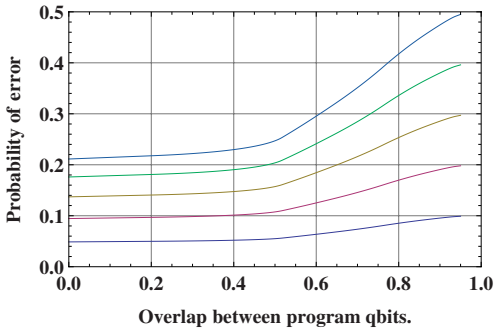

Fig. 2. (Color online) Probable errors for known overlap between program qbits. $\eta_1 = 0.1$ (lower curve) to $\eta_1 = 0.5$ (upper curve) in steps of 0.1.

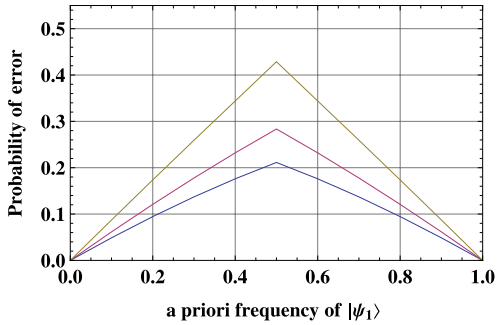

Fig. 3. (Color online) Probability of error against a priori frequency for overlap = 0 (upper curve), 0.4 (centre curve), and 0.8 (lower curve).

a priori probabilities. The left-hand border describes the system when the two program qbits are orthogonal (zero overlap) and shows that the worst discrimination, for all overlaps, occurs when $\eta_1 = 1/2$. For values of overlap close to 1, a nearly optimal strategy is to choose the most likely value of the data qbit, depending on η_1. The error probability for $\eta_1 = 1/2$ and zero overlap ($\beta = \pi$) coincides with the analytic solution presented at the end of the last section. Figure 3 gives a different view of some of the same data. With each value of overlap, the probability of error increases almost linearly to a maximum when the a priori expectations of the two states are equal.

4.2 Unambiguous discrimination for a Triad with known overlap

Finding the failure rate for unambiguous discrimination uses the same analysis as was presented in [13] and summarised in the previous section. The only difference is that whereas the Hunter group found an average overlap of the program qbits of $\sqrt{1/2}$ we can use specific values. Figure 4 shows how the success rate depends on η_1 for various fixed overlaps, using the formula

$$P = \frac{2}{3}\left(1 - \sqrt{(\eta_1\eta_2)}\right)\left(1 - \overline{|\langle\psi_1|\psi_3\rangle|^2}\right). \tag{38}$$

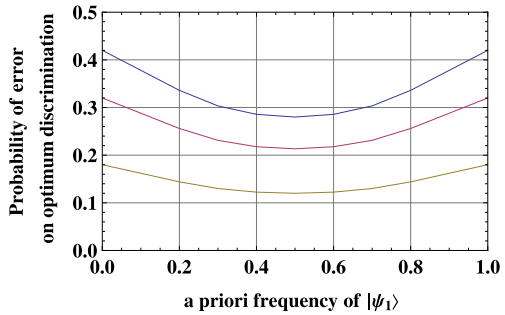

Fig. 4. (Color online) Probability of success in unambiguous discrimination against a priori frequency for overlap = 0 (upper curve), 0.4 (centre curve), and 0.8 (lower curve).

5 The great circle case

In the great circle case, we have a priori knowledge that both the program qbits lie on a *given* great circle of the Bloch sphere. This condition is important, as any two randomly selected different points on the Bloch sphere define *some* great circle, but we can exploit knowledge of the specific great circle in the choice of our measurement.

Another point to note is that any given great circle can be transformed to coincide with the equator, or with what we might call the extended Greenwich Meridian, just by rotating it about the sphere. It follows that the error rate for *all* given great circles will be the same.

Taking the great circle to be the extended Greenwich Meridian for which the azimuthal angle is either 0 or π, we can incorporate both possibilities by writing

$$|\psi_1\rangle = \cos(\alpha/2)|0\rangle + \sin(\alpha/2)|1\rangle$$
$$|\psi_3\rangle = \cos(\gamma/2)|0\rangle + \sin(\gamma/2)|1\rangle \tag{39}$$

and allowing α and γ to take values in the range 0 to 2π. Following the now accustomed pattern, we write

$$|\Psi_1\rangle = |\psi_1\rangle|\psi_1\rangle|\psi_3\rangle$$
$$\hat{\rho}_1 = |\psi_1\rangle|\psi_1\rangle\langle\psi_1|\langle\psi_1| \otimes |\psi_3\rangle\langle\psi_3|$$
$$= \hat{\lambda}_1 \otimes \hat{\mu}_1. \tag{40}$$

Both $\hat{\lambda}_1$ and $\hat{\mu}_1$ must be averaged on our great circle (rather than the surface of the full Bloch sphere). Averaging $\hat{\lambda}_1$ over a circle defined by $(0 \le \alpha \le 2\pi)$ gives the density matrix:

$$\overline{\hat{\lambda}}_1 = \frac{1}{8}\begin{pmatrix} 3 & 0 & 0 & 0 \\ 0 & 1 & 1 & 0 \\ 0 & 1 & 1 & 0 \\ 0 & 0 & 0 & 3 \end{pmatrix}. \tag{41}$$

Similarly, averaging $\hat{\mu}_1$ over a circle defined by $(0 \le \gamma \le 2\pi)$ leads to:

$$\overline{\hat{\mu}}_1 = \frac{1}{2}\begin{pmatrix} 1 & 0 \\ 0 & 1 \end{pmatrix}. \tag{42}$$

It then follows that

$$\overline{\hat{\rho}}_2 = \overline{\hat{\lambda}} \otimes \overline{\hat{\mu}}. \tag{43}$$

The density operator $\overline{\hat{\rho}}_2$ is worked out by a similar method:

$$\overline{\hat{\rho}}_2 = \overline{\hat{\mu}} \otimes \overline{\hat{\lambda}}. \tag{44}$$

The explicit forms of these two density operators are given in Appendix.

5.1 Minimum error for a Triad confined to a known great circle

The minimum-error strategy for distinguishing between these states requires us to find the eigenvalues of $\hat{\Lambda}$, given in (12). For equal prior probabilities ($\eta_1 = 1/2$) we find the minimum error probability P.E. ≈ 0.323.

5.2 Unambiguous discrimination for a Triad confined to a known great circle

When the two program qbits are confined to a great circle, their average overlap is $\sqrt{1/2}$. We conclude that the probability of failure Q_F is

$$Q_F = \frac{2 + \sqrt{\eta_1 \eta_2}}{3}, \tag{45}$$

as in the general case described by the Hunter group.

For unambiguous discrimination, knowledge that both program qbits are on a known great circle makes no difference to the probability of failure, as the overlap of the two program qbits is the same as when their positions on the Bloch sphere are unrestricted.

6 The 'polar cap' case

The polar cap configuration posits a Triad in which one program qbit is located in a cap centred on the north pole of the Bloch sphere, and the other in a cap centred on the south pole. Both caps are the same size, bounded by lines of latitude defined by the angle θ, as shown in Figure 5.

6.1 Minimum error in the polar cap case

The northern program qbit may be written as

$$|\psi_N\rangle = \cos(\beta/2)|0\rangle + e^{i\alpha}\sin(\beta/2)|1\rangle \tag{46}$$

where $(0 \le \beta \le \theta)$. Similarly, the southern program qbit is

$$|\psi_S\rangle = \cos(\delta/2)|0\rangle + e^{i\gamma}\sin(\delta/2)|1\rangle \tag{47}$$

where $(\pi - \theta \le \delta \le \pi)$. The two possible states of the discriminator are:

$$|\Psi_1\rangle = |\psi_N\rangle|\psi_N\rangle|\psi_S\rangle$$
$$|\Psi_2\rangle = |\psi_N\rangle|\psi_S\rangle|\psi_S\rangle. \tag{48}$$

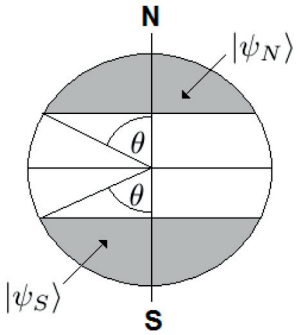

Fig. 5. Locations of the two program qbits for the 'Polar cap' configuration.

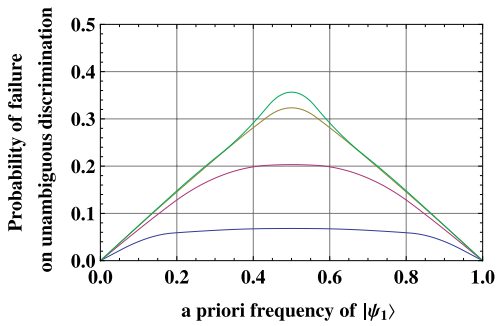

Fig. 6. (Color online) Probable error for $\theta = \pi/4$ (bottom curve) to $\theta = \pi/$ (top curve) in steps of $\pi/4$.

The density matrix for the first of these two states is obtained as before, by averaging the states over the relevant cap. If we define

$$\hat{\mu} = |\psi_N\rangle|\psi_N\rangle\langle\psi_N|\langle\psi_N|$$
$$\hat{\lambda} = |\psi_S\rangle\langle\psi_S| \tag{49}$$

then averaging gives

$$\overline{\hat{\mu}}_1 = \frac{1}{\kappa}\int_0^{2\pi} d\psi \int_0^{\theta} d\beta \sin\beta \hat{\mu}$$
$$= \begin{pmatrix} a & 0 & 0 & 0 \\ 0 & b & b & 0 \\ 0 & b & b & 0 \\ 0 & 0 & 0 & c \end{pmatrix}, \tag{50}$$

where $\kappa = 2\pi(1-\cos\theta)$ is the surface area of the cap and

$$a = \frac{1}{\kappa}\int_0^{2\pi} d\alpha \int_0^{\theta} d\beta \cos^4(\beta/2)\sin(\beta)$$
$$= \frac{2}{3}\left(\frac{1-\cos^6(\theta/2)}{1-\cos\theta}\right) \tag{51}$$

$$b = \frac{1}{\kappa}\int_0^{2\pi} d\alpha \int_0^{\theta} d\beta \cos^2(\beta/2)\sin^2(\beta/2)\sin(\beta)$$
$$= 4\left(\frac{\frac{1}{4}\sin^4(\theta/2) - \frac{1}{6}\sin^6(\theta/2)}{1-\cos\theta}\right) \tag{52}$$

$$c = \frac{1}{\kappa}\int_0^{2\pi} d\alpha \int_0^{\theta} d\beta \sin^4(\beta/2)\sin(\beta)$$
$$= \frac{2}{3}\left(\frac{\sin^6(\theta/2)}{1-\cos\theta}\right). \tag{53}$$

Similarly, averaging $\hat{\lambda}$ over the southern cap gives

$$\overline{\hat{\lambda}}_1 = \frac{1}{\kappa}\int_0^{2\pi} d\psi \int_{\pi-\theta}^{\pi} d\delta \sin\delta \hat{\lambda} \tag{54}$$

$$= \begin{pmatrix} d & 0 \\ 0 & e \end{pmatrix} \tag{55}$$

where

$$d = \frac{1}{\kappa}\int_0^{2\pi} d\gamma \int_{\pi-\theta}^{\pi} d\delta \cos^2(\delta/2)\sin(\delta)$$
$$= \left(\frac{\sin^4(\theta/2)}{1-\cos\theta}\right) \tag{56}$$

$$e = \frac{1}{\kappa}\int_0^{2\pi} d\gamma \int_{\pi-\theta}^{\pi} d\delta \sin^2(\delta/2)\sin(\delta)$$
$$= \left(\frac{1-\cos^4(\theta/2)}{1-\cos\theta}\right). \tag{57}$$

Tensor multiplication of these two matrices gives the density operator:

$$\overline{\hat{\rho}}_1 = \overline{\hat{\mu}} \otimes \overline{\hat{\lambda}}. \tag{58}$$

The second density operator is obtained in the same manner:

$$\overline{\hat{\rho}}_2 = \overline{\hat{\lambda}} \otimes \overline{\hat{\mu}}. \tag{59}$$

Both matrices, expressed in terms of the variables a to e, are given in Appendix.

Figure 6 shows how the probable error varies with η_1, for a selection of values of θ. It is worth noting, as a check, that when $\theta = \pi$, and the positions of the program qbits are unrestricted, the results are identical with those of the Hunter group for a similar configuration.

6.2 Unambiguous discrimination for a Triad in the polar cap case

As before, the success rate of unambiguous discrimination is determined only by the ratio of η_1 and η_2, and by the overlap of the two program qbits. In the polar cap case the overlap changes with the angle θ in a non-linear manner, shown in Figure 7. The corresponding success rates S are displayed in Figure 8, using the formula

$$S = 1 - \frac{2}{3}\left(1 - \sqrt{(\eta_1\eta_2)}\right)\left(1 - \overline{|\langle\psi_1|\psi_3\rangle|^2}\right). \tag{60}$$

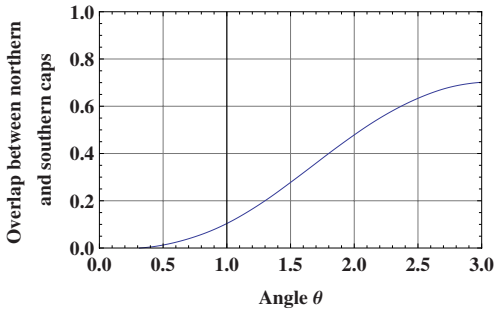

Fig. 7. (Color online) Overlap between polar caps for values of θ.

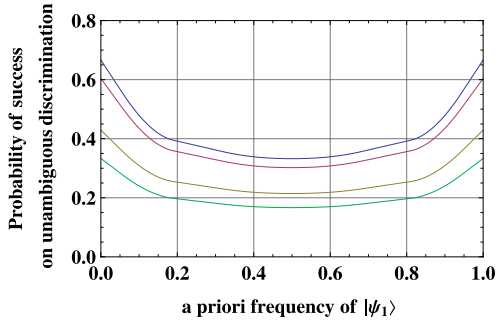

Fig. 8. (Color online) Probable error for $\theta = \pi/4$ (top curve) to $\theta = \pi$ (bottom curve) in steps of $\pi/4$.

7 Conclusions

We have investigated the error rates in discriminating the two possible states of a Triad, when certain types of additional information are available. In practice, this could often be the case. For example, if the two program qbits are coded as photons with different linear polarisations, they will lie on a great circle of the Bloch sphere.

We can report a number of findings, first for mimimum error measurements:

- When the two program qbits of a Triad are orthogonal, and the two possible states are equally likely, the probability of error is less than if they were selected randomly (0.211 as opposed to 0.356). The minimum error rate rises monotonically as the overlap between the qbits increases.
- If both program qbits are on the same (given) great circle, the expected minimum error rate is 0.323.
- If the program qbits are confined to 'caps' centred in antipodeal points on the Bloch sphere, the error rate grows as the areas increase in size. In particular, if each area covers just half the Bloch sphere, and $\eta_1 = \eta_2 = \frac{1}{2}$, the error rate in recognition is 0.203.

Our results on minimum error rates broadly confirm our expectations – that additional classical information about a Triad can improve the successful discrimination rate. An interesting result is that the error rate for the case when the two program qbits are in the northern and southern hemispheres of the Bloch sphere is actually slightly *lower* than the rate for orthogonal program qbits. It seems that absolute positional information carries more weight than relational data.

Second, for unambiguous measurements:

In all cases, the failure rate is disappointingly large. However, the rate is improved when the data qbits are known to have a small overlap, or are confined to small areas about antipodeal poles. The knowledge that the program qbits are confined to a given great circle makes no difference to error rate.

This work was supported by the UK Engineering and Physical Research Council, the Royal Society and the Wolfson Foundation. We specially wish to thank the reviewers for their comments on the first version of this paper, and for pointing out a significant error in our computations.

Appendix

The appendix gives the density matrices in full for the various cases of known additional information.

A.1 Hunter group's analysis

$$\overline{\hat{\rho}}_1 = \overline{\hat{\lambda}}_1 \otimes \overline{\hat{\mu}}_1 = \frac{1}{12}\begin{pmatrix} 2&0&0&0&0&0&0&0\\ 0&2&0&0&0&0&0&0\\ 0&0&1&0&1&0&0&0\\ 0&0&0&1&0&1&0&0\\ 0&0&1&0&1&0&0&0\\ 0&0&0&1&0&1&0&0\\ 0&0&0&0&0&0&2&0\\ 0&0&0&0&0&0&0&2 \end{pmatrix}. \quad \text{(A.1)}$$

This density matrix applies to the first of the two states, where the first and the second qbits are identical. Similarly, if the second and third qbits are identical,

$$\overline{\hat{\rho}}_2 = \frac{1}{12}\begin{pmatrix} 2&0&0&0&0&0&0&0\\ 0&1&1&0&0&0&0&0\\ 0&1&1&0&0&0&0&0\\ 0&0&0&2&0&0&0&0\\ 0&0&0&0&2&0&0&0\\ 0&0&0&0&0&1&2&0\\ 0&0&0&0&0&1&1&0\\ 0&0&0&0&0&0&0&2 \end{pmatrix}. \quad \text{(A.2)}$$

A.2 Finding density matrices for constant overlap of program qbits

$$|p\rangle = \cos(\beta/2)\begin{pmatrix} \cos^3(\theta/2) & |000\rangle\\ +e^{i\psi}\sin(\theta/2)\cos^2(\theta/2) & |001\rangle\\ +e^{i\psi}\sin(\theta/2)\cos^2(\theta/2) & |010\rangle\\ +e^{i\psi}\sin(\theta/2)\cos^2(\theta/2) & |100\rangle\\ +e^{2i\psi}\sin^2(\theta/2)\cos(\theta/2) & |011\rangle\\ +e^{2i\psi}\sin^2(\theta/2)\cos(\theta/2) & |101\rangle\\ +e^{2i\psi}\sin^2(\theta/2)\cos(\theta/2) & |110\rangle\\ +e^{3i\psi}\sin^3(\theta/2) & |111\rangle \end{pmatrix}, \quad \text{(A.3)}$$

$$|q_1\rangle = \sin(\beta/2)\begin{pmatrix} \cos^2(\theta/2)\sin(\theta/2) & |000\rangle \\ -e^{i\psi}\cos^3(\theta/2) & |001\rangle \\ +e^{i\psi}\cos(\theta/2)\sin^2(\theta/2) & |010\rangle \\ +e^{i\psi}\cos(\theta/2)\sin^2(\theta/2) & |100\rangle \\ -e^{2i\psi}\cos^2(\theta/2)\sin(\theta/2) & |011\rangle \\ -e^{2i\psi}\cos^2(\theta/2)\sin(\theta/2) & |101\rangle \\ +e^{2i\psi}\sin^3(\theta/2) & |110\rangle \\ -e^{3i\psi}\cos(\theta/2)\sin^2(\theta/2) & |111\rangle \end{pmatrix}, \tag{A.4}$$

$$|q_2\rangle = \sin(\beta/2)\begin{pmatrix} \cos^2(\theta/2)\sin(\theta/2) & |000\rangle \\ +e^{i\psi}\cos(\theta/2)\sin^2(\theta/2) & |001\rangle \\ +e^{i\psi}\cos(\theta/2)\sin^2(\theta/2) & |010\rangle \\ -e^{i\psi}\cos^3(\theta/2) & |100\rangle \\ +e^{2i\psi}\sin^3(\theta/2) & |011\rangle \\ -e^{2i\psi}\cos^2(\theta/2)\sin(\theta/2) & |101\rangle \\ -e^{2i\psi}\cos^2(\theta/2)\sin(\theta/2) & |110\rangle \\ -e^{3i\psi}\cos(\theta/2)\sin^2(\theta/2) & |111\rangle \end{pmatrix}. \tag{A.5}$$

Note that the computational states are not listed in the order of the corresponding binary numbers, but are grouped according to the number of $|1\rangle s$ they contain; this generates density matrices with compact sub-matrices on the main diagonal and zeros elsewhere.

Each term in this expansion is the product of the appropriate elements of $|0\rangle$ and $|1\rangle$. For example, the coefficient of $|101\rangle$ in the state vector $|q_1\rangle$ is the product of: $e^{i\psi}\sin(\theta/2)|1\rangle$, $\cos(\theta/2)|0\rangle$, and $-e^{i\psi}\cos(\theta/2)|1\rangle$

$$\frac{1}{4\pi}\int_S AdS = \frac{1}{12}\begin{pmatrix} 3&0&0&0&0&0&0&0\\ 0&1&1&1&0&0&0&0\\ 0&1&1&1&0&0&0&0\\ 0&1&1&1&0&0&0&0\\ 0&0&0&0&1&1&1&0\\ 0&0&0&0&1&1&1&0\\ 0&0&0&0&1&1&1&0\\ 0&0&0&0&0&0&0&3 \end{pmatrix}, \tag{A.6}$$

$$\frac{1}{4\pi}\int_S BdS = \frac{1}{12}\begin{pmatrix} 1&0&0&0&0&0&0&0\\ 0&3&-1&-1&0&0&0&0\\ 0&-1&1&1&0&0&0&0\\ 0&-1&1&1&0&0&0&0\\ 0&0&0&0&1&1&-1&0\\ 0&0&0&0&1&1&-1&0\\ 0&0&0&0&-1&-1&3&0\\ 0&0&0&0&0&0&0&1 \end{pmatrix}, \tag{A.7}$$

$$\frac{1}{4\pi}\int_S CdS = \frac{1}{12}\begin{pmatrix} 1&0&0&0&0&0&0&0\\ 0&1&1&-1&0&0&0&0\\ 0&1&1&-1&0&0&0&0\\ 0&-1&-1&3&0&0&0&0\\ 0&0&0&0&3&-1&-1&0\\ 0&0&0&0&-1&1&1&0\\ 0&0&0&0&-1&1&1&0\\ 0&0&0&0&0&0&0&1 \end{pmatrix}. \tag{A.8}$$

A.3 Density matrices for the great circle case

$$\overline{\hat{\rho}}_1 = \overline{\hat{\lambda}}_1 \otimes \overline{\hat{\mu}}_1 = \frac{1}{16}\begin{pmatrix} 3&0&0&0&0&0&0&0\\ 0&3&0&0&0&0&0&0\\ 0&0&1&0&1&0&0&0\\ 0&0&0&1&0&1&0&0\\ 0&0&1&0&1&0&0&0\\ 0&0&0&1&0&1&0&0\\ 0&0&0&0&0&0&3&0\\ 0&0&0&0&0&0&0&3 \end{pmatrix}; \tag{A.9}$$

$$\overline{\hat{\rho}}_2 = \overline{\hat{\mu}}_1 \otimes \overline{\hat{\lambda}}_1 = \frac{1}{16}\begin{pmatrix} 3&0&0&1&0&0&0&0\\ 0&1&1&0&0&0&0&0\\ 0&1&1&0&0&0&0&0\\ 1&0&0&3&0&0&0&0\\ 0&0&0&0&3&0&0&0\\ 0&0&0&0&0&1&1&0\\ 0&0&0&0&0&1&1&0\\ 0&0&0&0&1&0&0&3 \end{pmatrix}. \tag{A.10}$$

A.4 Density matrices for the polar cap configuration

$$\overline{\hat{\rho}}_1 = \overline{\hat{\mu}} \otimes \overline{\hat{\lambda}} = \begin{pmatrix} ad&0&0&0&0&0&0&0\\ 0&ae&0&0&0&0&0&0\\ 0&0&bd&0&bd&0&0&0\\ 0&0&0&be&0&be&0&0\\ 0&0&bd&0&bd&0&0&0\\ 0&0&0&be&0&be&0&0\\ 0&0&0&0&0&0&cd&0\\ 0&0&0&0&0&0&0&ce \end{pmatrix}; \tag{A.11}$$

$$\overline{\hat{\rho}}_2 = \overline{\hat{\lambda}} \otimes \overline{\hat{\mu}} = \begin{pmatrix} ce&0&0&0&0&0&0&0\\ 0&be&be&0&0&0&0&0\\ 0&be&be&0&0&0&0&0\\ 0&0&0&ae&0&0&0&0\\ 0&0&0&0&cd&0&0&0\\ 0&0&0&0&0&bd&bd&0\\ 0&0&0&0&0&bd&bd&0\\ 0&0&0&0&0&0&0&ad \end{pmatrix}. \tag{A.12}$$

References

1. J.A. Bergou, V. Bužek, E. Feldman, U. Herzog, M. Hillery, Phys. Rev. A **73**, 062334 (2006)
2. E. Morrison, P. Morrison, *Charles Babbage's Papers* (Dover Publications, New York, 1962)
3. D. Hanneke, J.P. Home, J.D. Jost, J.M. Amini, D. Leibfried, D.J. Wineland, Nature Phys., DOI:10.1038/nphys1453
4. S.M. Barnett, *Quantum Information* (Oxford University Press, Oxford, 2009)
5. S.M. Barnett, S.Croke, Adv. Opt. Photon **1**, 238 (2009)
6. S.M. Barnett, A. Chefles, I. Jex, Phys. Lett. A **307**, 195 (2003)
7. I. Jex, G. Alber, S.M. Barnett, A. Delgado, Fortschr. Phys. **51**, 172 (2003)
8. M.A. Nielsen, I.L. Chuang, *Quantum Computation and Quantum Information* (Cambridge University Press, New York, 2000)
9. J. von Neumann, *Mathematical Foundations of Quantum Mechanics* (Princeton University Press, 1957)
10. M. Sedlak, M. Ziman, V. Bužek, M. Hillery, Phys. Rev. A **77**, 042304 (2008)
11. M. Kleinmann, H. Kampermann, D. Bruß, Phys. Rev. A **72**, 032308, (2005)
12. C.W. Helstrom, *Quantum detection and estimation theory* (Academic Press, New York, 1976)
13. J.A. Bergou, M. Hillery, Phys. Rev. Lett. **94**, 160501 (2005)